International Journal of Automotive Technology, Vol. ?, No. ?, pp. ?–?(year)

Serial#Given by KSAE

Adaptive sliding mode control of lateral stability of four wheel hub electric vehicles

Shou-Tao Li[1)], Hui Liu[1)], Di Zhao[1)], Qiu-Yuan Li[1)], Yan-Tao Tian[1)] , De-Jun Wang[1)] and Ding-Li Yu[2)#]

[1)] College of Communications Engineering, Jilin University, Changchun 130022, China
[2)] Dept of Electrical Engineering, Liverpool John Moores University, Liverpool L3 3AF, U.K.
Corresponding author (D.Yu@ljmu.ac.uk)

ABSTRACT– Some physical parameters of a hub motor-driven four-wheel electric vehicle will change when the vehicle turns or maneuvers and the parameter change is caused by the change of the driving conditions. An adaptive sliding mode control is proposed in this paper to maintain the vehicle's stability by compensating for the change of these parameters. The control parameter being adapted is the converging rate of the system state towards the sliding mode. As the Lyapunov method is used, so both the vehicle stability and adaptive rate convergence are guaranteed. Moreover, the hierarchical control structure is adopted for this vehicle stability control system. The above adaptive sliding model control forms the upper-layer; while the lower-layer control is to distribute the upper torque to the four wheels in an optimal way, subject to several constraints. In addition, the best feasible reference of the yaw velocity and the lateral mass angle of the center of mass are obtained and used in the control system. The developed method is simulated under the CarSim/MATLAB co-simulation environment to evaluate the system performance. The simulation results are compared with the non-adaptive existing sliding mode control, and show that the proposed method is superior under different conditions.

KEY WORDS: electric vehicle, vehicle stability, adaptive sliding mode control, parameter uncertainty, torque distribution.

1. INTRODUCTION

In recent years, new energy is rapidly developed to cope with global energy crisis and serious air pollution. Electric vehicles become the most potential direction of transportation tools (Fabio,2013). Vehicle stability is affected by many factors such as vehicle structural parameters, driving speed and steering angle, etc. (Wolfgang et al., 1993). Specifically, in low speed and low coefficient of adhesion or high speed and high attachment road conditions, the load on vehicle rear axle will transit to the front axle, while the load on the inner wheel will transit to the outside wheel. These load transition will make some of the vehicle structure parameters, such as the lateral stiffness, continuously change (Le and Chen, 2016). When this happen, in the extreme case, the vehicle may become unstable and run out from the expected driving path, which may lead to safety problem.

In the study of vehicle safety, active safety is increasingly becoming the core of automotive safety research. The vehicle handling stability becomes the focus of recent research in this area (Milad,2017). At present, the combination of electronic stability (ESP) and intelligent-assisted cruise control (ACC) can prevent accidents in automobiles and form the fundamental techniques of unmanned vehicles (Hansung, 2009). There are some control problems for vehicle handling stability, such as tire non-linearity problems. Liang Li et al. (2015) proposed a hierarchical control with nonlinear tire constraints to tackle the tire nonlinearity problem. For steering stability, several methods including adaptive neural network sliding mode control (Wang et al., 2016), model predictive control (Choi et al., 2014), sliding mode variable structure control (Tchamna and Youn, 2013), linear quadratic regulator (LQR) control (Rler, 2015) and others. In addition, impacts of some parameter uncertainty on vehicle stability has been investigated and some emerging research on this issue becomes a research hotspot. The side stiffness of tires is the main source of parameter uncertainty. Firstly, vertical load of the tire is continuously shifted forward and backward with the driving conditions during the driving of the vehicle. As a result, the lateral stiffness of the tire changes

* *Corresponding author*. e-mail: D.Yu@ljmu.ac.uk

nonlinearly with the vertical load. Secondly, the stiffness of the side-by-side tire is affected by the inflation pressure of the tire and increases with the increase of the pressure. But, the stiffness of the side pressure does not change accordingly and becomes saturated. Thirdly, the tire size, the structural parameters and the detached pavement adhesion coefficient are all have a significant effect on Partial stiffness (Akio, 2009). However, the side stiffness of tires is difficult to obtain directly from the non-linear tire model. Some researchers tried to estimate this parameter using the recursive Least Squares algorithm. The obtained lateral stiffness was then used to estimate the side slip angle of the center of mass (Lian, 2015). Moreover, the accurate lateral stiffness not only enables accurate estimation of slip angle, should also improve the steering stability. Based on this idea, Kazemi (2010) proposed a nonlinear adaptive sliding mode control for steer-by-wire control system to improve steering stability and reduce jitter caused by uncertain parameters such as lateral stiffness. Some researchers treated the uncertainty of the lateral stiffness as a kind of disturbance, and used the robust H_∞ output feedback control to track the desired path, while considering the lateral stiffness as a kind of time-varying and uncertain parameters in the modelling (Rongrong, 2016). Another research used the H_∞ observer to improve the stability under uncertain parameters, where the uncertainties of the robust H∞ controller parameters are optimized by transforming the parameter uncertainty into a perturbation matrix (Zhang, 2013). This controller is robust to the parameter uncertainty but the computing load is high. In new energy vehicles, four-wheel, independently-driven hub electric vehicles control four tires directly. The fast response of the electric motor facilitates direct yaw moment control (DYC) (Yu, 2016). The four-wheel hub motor-driven electric vehicle achieves the goal of controlling the yaw stability through coordinated control of the driving and braking torques of the four wheels (Hasan and Mehran, 2015). Zhao et al. (2015) utilized nonlinear model predictive control algorithm for four-wheel independent torque distribution. Luo et al. (2015) proposed that longitudinal, lateral and vertical tire force coordination control distribute tire force to each wheel to solve non-convex optimization problem. Li et al. (2015) established an objective function to optimize the distribution of torque for four-wheel drive independent electric vehicles.

It is realized in our research that the time-varying feature of the tire stiffness not only affected by some parameters in an electric vehicle, also affected by many factors. This is the motivation behind this research. In this paper, a hierarchical control structure is proposed with the upper layer using adaptive sliding mode control to maintain vehicle stability under system uncertainty, while the lower layer distribute optimally the load torque to the four wheels. Specifically, an adaptive law is derived using the Lyapunov method and is added to a traditional sliding mode control for the uncertainty of side stiffness to ensure the stability of the vehicle. The system makes the decision according to the state of the controlled system and the error of the yaw angle and yaw rate of the center of mass. The controller updates the control action according to the adaptive law to ensure the accurate tracking of both yaw velocity and the lateral mass angle of the center of mass, under the applied constraints. The adaptive sliding mode controller can automatically adapt to different factors caused by changes in the deflection of the stiffness. The lower layer control is to distribute the upper torque to the wheels, comparing with the existing distribution method that is mainly based on a certain rules of single wheel distribution or average distribution. It is worth mentioning that the road surface adhesion of the tire is not fully utilized in the proposed control system, the main reason for which is we found out that the road surface adhesion of the tire is closely related to the stability margin of the vehicle. Full use of the road surface adhesion will take the risk of vehicle unstable. In addition, the maximum torque of the motor constraints, in the extreme braking conditions, cannot meet the control torque demand, which is improved by adding hydraulic braking force in this paper.

2. VEHICLE MODELLING

2.1. Body dynamics

A dynamic model of the vehicle is derived for the dynamics of longitudinal, lateral and yaw in this paper using the Newton-Euler method (Nam, 2014). The following assumptions have been made to simplify the model:

(1) The vehicle moves on the horizontal road.

(2) The left and right wheels of the front axle have the same turning angle, i.e. $\delta_f = \delta$; $\delta_r = 0$.

(3) Rolling movement is neglected.

(4) The air resistance is not considered.

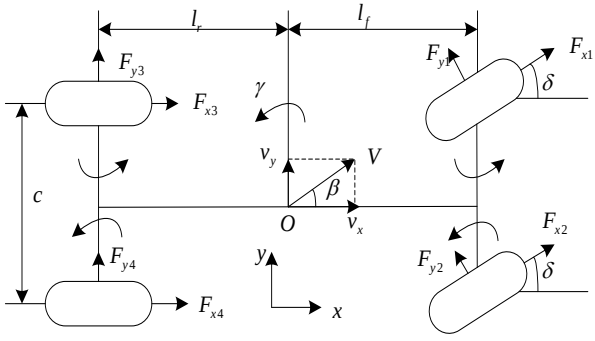

Fig. 1 Seven degrees of freedom vehicle model

The differential equations for longitudinal, lateral and yaw movements on the XY plane are derived as follows:

Longitudinal equation of motion:

$$m\ddot{x} = (F_{x1} + F_{x2})\cos\delta + F_{x3} + F_{x4} - (F_{y1} + F_{y2})\sin\delta + m\gamma\dot{y} \quad (1)$$

Lateral movement:

$$m\ddot{y} = (F_{y1} + F_{y2})\cos\delta + F_{y3} + F_{y4} + (F_{x1} + F_{x2})\sin\delta - m\gamma\dot{x} \quad (2)$$

Yaw movement:

$$\begin{aligned} I_Z\dot{\gamma} = {} & \frac{c}{2}\left[(F_{x2} - F_{x1})\cos\delta + (F_{y1} - F_{y2})\sin\delta\right] + \frac{c}{2}(F_{x4} - F_{x3}) \\ & + l_f\left[(F_{y1} + F_{y2})\cos\delta + (F_{x1} + F_{x2})\sin\delta\right] - l_r(F_{y3} + F_{y4}) \end{aligned} \quad (3)$$

where I_Z is the moment of inertia around Z axis of the vehicle body; $F_{xi}(\mathrm{i} = 1,2,3,4)$ can be obtained from the driving force observer (DFO) designed by the kinetic equation of the wheel rotation (Nam, 2015),

$$F_{xi} = \frac{\omega_D}{s + \omega_D}\left(\frac{T_i - I_\omega\omega_i s}{r}\right) \quad (4)$$

here, ω_i are four wheel angular velocities; T_i is wheel motor torque ; ω_D is the cut-off frequency of the low pass filter. Four wheel motion equations are

$$F_{xi}R + J_i\dot{\omega}_i - T_{ti} + T_{bi} = 0 \qquad i = 1,\cdots,4 \quad (5)$$

When vehicle moves the vertical load will affect the well, and the vertical load was affected by the vehicle moving states. Then, the load transfer between axis will occur. The wheel dynamic model is required to calculate both rotation and the vertical load of each wheel, so that provides accurate vertical load for the tire force to be computed. Following equations are used to calculate the vertical load for the wheels:

$$\begin{aligned} F_{z1} &= \frac{1}{2}mg\cdot\frac{l_r}{l_f + l_r} - \frac{1}{2}\frac{ma_x\cdot h}{l_f + l_r} - ma_y\cdot\frac{l_r}{l_f + l_r}\cdot\frac{h}{c} \\ F_{z2} &= \frac{1}{2}mg\cdot\frac{l_r}{l_f + l_r} - \frac{1}{2}\frac{ma_x\cdot h}{l_f + l_r} + ma_y\cdot\frac{l_r}{l_f + l_r}\cdot\frac{h}{c} \\ F_{z3} &= \frac{1}{2}mg\cdot\frac{l_f}{l_f + l_r} + \frac{1}{2}\frac{ma_x\cdot h}{l_f + l_r} - ma_y\cdot\frac{l_f}{l_f + l_r}\cdot\frac{h}{c} \\ F_{z4} &= \frac{1}{2}mg\cdot\frac{l_f}{l_f + l_r} + \frac{1}{2}\frac{ma_x\cdot h}{l_f + l_r} + ma_y\cdot\frac{l_f}{l_f + l_r}\cdot\frac{h}{c} \end{aligned} \quad (6)$$

Where m is the mass of the vehicle; x is the longitudinal displacement; y is the lateral displacement; l_f l_r are the distances from the centroid of the vehicle to the front and rear axles; c is the car wheelbase; γ is the yaw angular velocity; β is the centroid lateral deflection. Also, $F_{x1}, F_{x2}, F_{x3}, F_{x4}$ are the longitudinal force of the front left, front right, rear left and rear right tires of the vehicle; $F_{y1}, F_{y2}, F_{y3}, F_{y4}$ are the lateral force of these tires; δ_f δ_r are front wheel angle and rear wheel angle; R is the wheel radius; $F_{zi}(\mathrm{i} = 1,2,3,4)$ is vehicle vertical load.

2.2. Two degrees of freedom reference model

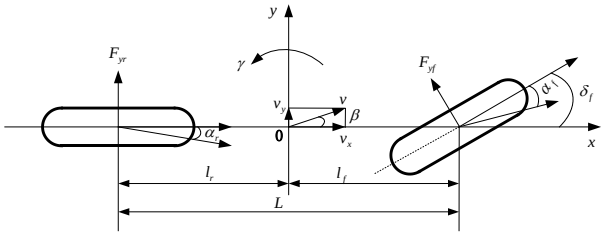

Fig. 2 Ideal two-degree-of-freedom vehicle model

In this paper, a two-degree-of-freedom (DOF) vehicle model displayed in Fig.2 is selected as the reference model of the driving trajectory. The obtained 2 DOF vehicle model is:

$$\begin{cases} m(\dot{v}_y + v_x\gamma) = (C_f + C_r)\beta + \dfrac{(l_fC_f - l_rC_r)}{v_x}\gamma - C_f\delta_f \\ I\dot{\gamma} = (l_fC_f - l_rC_r)\beta + \dfrac{(l_f^2C_f - l_r^2C_r)}{v_x}\gamma - C_f\delta_f \end{cases} \quad (7)$$

Here, v_x denotes the vehicle longitudinal velocity; v_y is the lateral velocity of the vehicle; C_f and C_r are the front and rear tire side stiffness; F_x is tire longitudinal force, F_y is lateral force of tire; f and r are the front and rear tires.

When the vehicle moving enters the steady state, γ is a constant value. At this time, $\dot{v}_y = 0, \dot{\gamma} = 0$. Substituting them into the first equation in (7) we get the ideal yaw velocity γ_{ideal} and the ideal centroid side angle β_{ideal} :

$$\gamma_{ideal} = \frac{v_x}{L(1 + Kv_x^2)}\delta_f \quad (8)$$

$$\beta_{ideal} = \left[\frac{l_r}{L(1 + Kv_x^2)} + \frac{ml_fv_x^2}{C_rL^2(1 + Kv_x^2)}\right]\delta_f \quad (9)$$

In the formula, $K=\frac{m}{L^2}\left(\frac{l_f}{C_r}-\frac{l_r}{C_f}\right)$ indicates the stability factor.

The lateral acceleration of the vehicle a_y cannot exceed the acceleration μ caused by the maximum adhesion coefficient of the road. Otherwise the vehicle will slip. Therefore, it is unreasonable to calculate the ideal value of the yaw angular velocity and the centroid lateral deflection based on the above equations. Thus, it is necessary to set the upper limit of the ideal value of the yaw angular velocity and the centroid lateral deflection as,

$$a_y \approx \frac{v_x^2}{R_1} = \gamma v_x \tag{10}$$

$$a_y \le \mu g \tag{11}$$

where R_1 is the turning radius. From the two equations we can see,

$$|\gamma| \le \left|\frac{\mu g}{v_x}\right| \tag{12}$$

According to (12), the upper limit of the yaw angular velocity and the centroid lateral deflection are:

$$\gamma_{d\max} = \frac{\mu g}{v_x} \tag{13}$$

$$\beta_{d\max} = \mu g\left(\frac{l_r}{v_x^2}+\frac{ml_f}{C_r L}\right) \tag{14}$$

The expected reference values of the yaw velocity and the lateral mass angle of the center of mass are finally obtained,

$$\gamma_d = \min\left(|\gamma_{ideal}|,|\gamma_{d\max}|\right)\cdot \mathrm{sgn}\left(\gamma_{ideal}\right) \tag{15}$$

$$\beta_d = \min\left(|\beta_{ideal}|,|\beta_{d\max}|\right)\cdot \mathrm{sgn}\left(\beta_{ideal}\right) \tag{16}$$

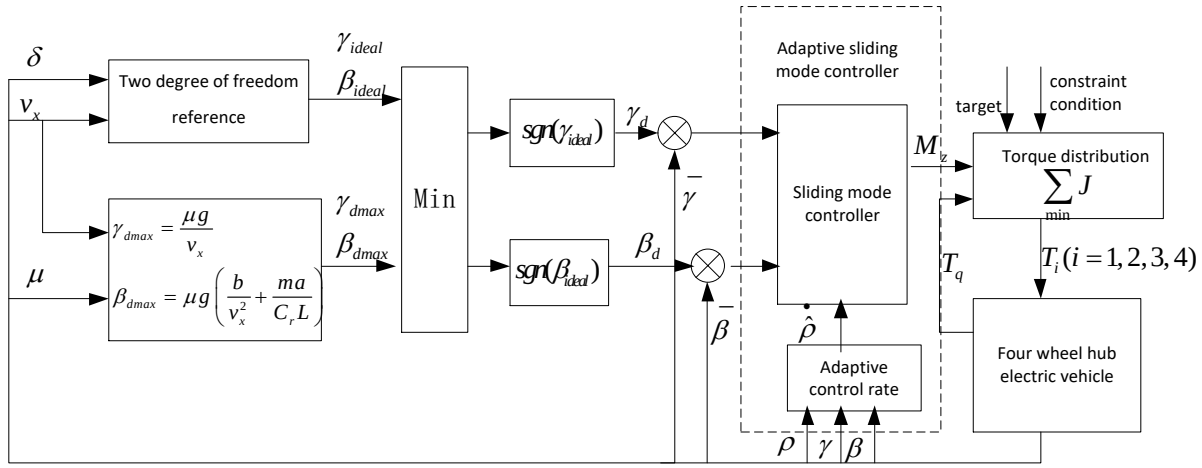

Fig. 3 Overall structure of the stability control system

3. OVERALL SYSTEM STRUCTURE

The overall structure of the stability control system is shown in Fig.3. The two DOF reference models use the steering wheel input δ and the current speed of the vehicle v_x to get the ideal yaw rate γ_{ideal} and side angle of the center of mass β_{ideal}. Then, considering the limitation of the adhesion coefficient of the pavement, the desired value of the ultimate lateral and yaw velocity of the center of mass is obtained. The sliding mode controller uses the reaching law to reduce the error of the side slip angle and yaw rate. According to the lateral stiffness function, an adaptive control law is designed and combined with the sliding mode controller to reduce the effects of parameter uncertainty. Then, an optimal torque allocation method is developed using the control target and input constraints. The proposed optimization problem is solved using the quadratic programming and distribute torque to four wheels to meet the needs of the required yaw moment M_z and the total required torque

T_q. In Fig.3 T_i (i=1, 2, 3, 4) are the driving / braking torque of four wheels.

4. VEHICLE STABILITY CONTROL

The motion tracking controller belongs to the upper controller of the system and calculates the yaw moment required for the stability of the vehicle according to the reference trajectory of the vehicle. When the vehicle runs under the limit condition, the rear axle load of the vehicle is transferred to the front axle and the inner wheel load is transferred to the outer wheel, which makes the structural parameters of the vehicle such as the lateral stiffness constantly changing. The traditional sliding mode variable structure controller cannot solve this problems, so an adaptive control is introduced to compensate for the system uncertainty.

The yaw movement is given as follows,

$$I_z\dot{\gamma} = l_f(F_{x1}+F_{x2})sin\delta + l_f\left(F_{y1}+F_{y2}\right)cos\delta - l_r\left(F_{y3}+F_{y4}\right) + M_z \tag{17}$$

And the direct yaw moment is

$$M_z = -l_f(F_{x1}+F_{x2})sin\delta - l_f\left(F_{y1}+F_{y2}\right)cos\delta + l_r\left(F_{y3}+F_{y4}\right) + I_z\dot{\gamma} \tag{18}$$

Considering linear tire force (Stratis and Mohsen, 2014) we have,

$$F_{yi} \approx -C_f\alpha_f \quad (i=1,2)$$
$$F_{yj} \approx -C_r\alpha_r \quad (j=3,4)$$
$$\alpha_f = \beta + \frac{l_f}{v_x}\gamma - \delta_f$$
$$\alpha_r = \beta - \frac{l_r}{v_x}\gamma$$

The above equations lead to,

$$F_{y1} + F_{y2} = -\alpha_f(C_1+C_2)$$
$$F_{y3} + F_{y4} = -\alpha_r(C_3+C_4)$$

Then, we have,

$$I_z\dot{\gamma} = -\frac{\gamma}{V_x}\left(l_f^2(C_1+C_2) + l_r^2(C_3+C_4)\right)cos\delta - l_r(C_3+C_4) + \delta l_f(C_1+C_2)cos\delta + l_f(F_{x1}+F_{x2})sin\delta + M_z \tag{19}$$

Let

$$C_1 = C_2 = C_f$$
$$C_3 = C_4 = C_r$$

$$\rho_1 = l_f^2(C_1+C_2)\cos\delta + l_r^2(C_3+C_4)$$
$$\rho_2 = l_f(C_1+C_2)\cos\delta - l_r(C_3+C_4)$$
$$\rho_3 = l_f(C_1+C_2)\cos\delta$$

The following two equations are derived,

$$I_z\dot{\gamma} = -\frac{\gamma}{V_x}\rho_1 - \beta\rho_2 + \delta\rho_3 + l_f(F_{x1}+F_{x2})sin\delta + M_z \tag{20}$$

$$M_z = \frac{\gamma}{V_x}\rho_1 + \beta\rho_2 - \delta\rho_3 - l_f(F_{x1}+F_{x2})sin\delta + I_z\dot{\gamma} \tag{21}$$

To track the desired centroid side slip angle and yaw rate, we design the weighted sum of the centroid side slip angle and yaw rate error as the sliding surface,

$$S = \gamma - \gamma_{ref} + \xi(\beta - \beta_{ref}) \tag{22}$$

Then, we have

$$\dot{S} = \dot{\gamma} - \dot{\gamma}_{ref} + \xi(\dot{\beta} - \dot{\beta}_{ref}) \tag{23}$$

The sliding mode convergence law is designed as an exponential convergence law,

$$\dot{S} = -k_pS - k_ssgn(S) \tag{24}$$

The k_p and k_s in the formula are positive control parameters. Then, using (21), (23) and (24), we obtain the control law as follows,

$$M_z = \frac{\gamma}{V_x}\rho_1 + \beta\rho_2 - \delta\rho_3 - l_f(F_{x1}+F_{x2})sin\delta - -I_z(k_pS + k_ssgn(S) - \dot{\gamma}_{ref} + \xi(\dot{\beta} - \dot{\beta}_{ref})) \tag{25}$$

Lemma 1. Considering the lateral and yaw motion of the vehicle (1)-(3), the sliding mode approach law (25) is designed under the condition of the linear tire force, which guarantees the asymptotic stability of the closed-loop system, $\lim_{t\to\infty}|S(t)| = 0$, such that the output converges to the expected reference trajectory.

Proof.

A Lyapunov function, $V_1 = \frac{1}{2}S^2$, is selected. Then,

$$\dot{V}_1 = S\dot{S} = S\left(-k_pS - k_ssgn(S)\right) = -k_pS^2 - k_s|S|$$

Since k_p and k_s are positive control parameters, therefore $\dot{V}_1 \le 0$. It then proves that the sliding mode control law is stable and satisfies $\lim_{t\to\infty}|S(t)| = 0$.

In the control law (25) parameters ρ_1, ρ_2 and ρ_3 are the functions of the wheelbase and the lateral stiffness. As shown in Fig.4, according to the lateral stiffness $C=\frac{F_y}{\alpha}$, we can see that the side force F_y and the side slip angle α changing with load change. Furthermore, under the same side deflection angle, the lateral stiffness increases with the increase of the vertical load of the tire; but under the same tire load, the side deflection is saturated when the side angle is too large, and the lateral stiffness decreases with the increase of lateral deflection angle. Therefore, ρ_1, ρ_2, and ρ_3 are uncertain parameters. In order to compensate the uncertainty of the system, the parameter adaptation for ρ_1, ρ_2, and ρ_3 is introduced here.

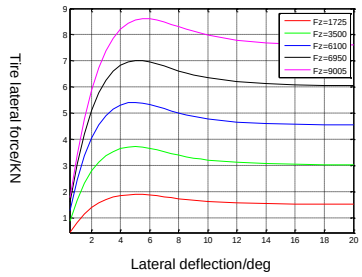

Fig. 4 Change of lateral deflection under different side angles and vertical loads

Let$\tilde{\rho}_i = \hat{\rho}_i - \rho_i$ (i = 1, 2, 3). The $\hat{\rho}_i$ is the estimated value of the unknown parameter, and $\tilde{\rho}_i$ is the error of parameter estimation. In order to compensate for the effects of the disturbance, the parameter adaptation law is designed as follows,

$$\dot{\hat{\rho}}_1 = -\frac{k_1 \gamma S}{I_z V_x} - \delta_1 \tilde{\rho}_1 \tag{26}$$

$$\dot{\hat{\rho}}_2 = -\frac{k_2 \beta S}{I_z} - \delta_2 \tilde{\rho}_2 \tag{27}$$

$$\dot{\hat{\rho}}_3 = -\frac{k_3 \delta S}{I_z} - \delta_3 \tilde{\rho}_3 \tag{28}$$

Among them, $k_i (i=1,2,3)$ are the adaptive gains and $\delta_i (i=1,2,3)$ are the undetermined coefficients.

The sliding mode control considering the parameter adaptation becomes,

$$M_z = \frac{\gamma}{V_x}\hat{\rho}_1 + \beta\hat{\rho}_2 - \delta\hat{\rho}_3 - l_f(F_{x1}+F_{x2})sin\delta - \\ -I_z(k_p S + k_s sgn(S) - \dot{\gamma}_{ref} + \xi(\dot{\beta} - \dot{\beta}_{ref})) \tag{29}$$

$$\dot{\gamma} = \frac{1}{I_z}(-\frac{\gamma}{V_x}\rho_1 - \beta\rho_2 + \delta\rho_3 + \frac{\gamma}{V_x}\hat{\rho}_1 + \beta\hat{\rho}_2 - \delta\hat{\rho}_3 - \\ -I_z(k_p S + k_s sgn(S) - \dot{\gamma}_{ref} + \xi(\dot{\beta} - \dot{\beta}_{ref})) \tag{30}$$

Theorem 1 Considering the lateral and yaw motions of the vehicle (1)-(3) under the condition of the linear tire force, any initial state off the sliding mode will be driven to on the sliding mode by the adaptive sliding mode control law (30), under the model uncertainty.

Proof. The Lyapunov function is designed as follows,

$$V_2 = \frac{1}{2}S^2 + \frac{1}{2k_1}\tilde{\rho}_1^2 + \frac{1}{2k_2}\tilde{\rho}_2^2 + \frac{1}{2k_3}\tilde{\rho}_3^2 \tag{31}$$

Then, the first order derivative of V_2 w.r.t. t is

$$\dot{V}_2 = S\dot{S} + \frac{1}{k_1}\tilde{\rho}_1\dot{\tilde{\rho}}_1 + \frac{1}{k_2}\tilde{\rho}_2\dot{\tilde{\rho}}_2 + \frac{1}{k_3}\tilde{\rho}_3\dot{\tilde{\rho}}_3$$

We have

$$\dot{S} = \frac{\gamma}{I_z V_x}\tilde{\rho}_1 + \frac{1}{I_z}\beta\tilde{\rho}_2 - \frac{\gamma 1}{I_z}\delta\tilde{\rho}_3 - k_p S - k_s sgn(S)$$

Leading to

$$\dot{V}_2 = S\left(\frac{\gamma}{I_z V_x}\tilde{\rho}_1 + \frac{1}{I_z}\beta\tilde{\rho}_2 - \frac{\gamma 1}{I_z}\delta\tilde{\rho}_3 - k_p S - k_s sgn(S)\right) \\ + \frac{1}{k_1}\tilde{\rho}_1\dot{\tilde{\rho}}_1 + \frac{1}{k_2}\tilde{\rho}_2\dot{\tilde{\rho}}_2 + \frac{1}{k_3}\tilde{\rho}_3\dot{\tilde{\rho}}_3$$

$$= -k_p S^2 - k_s|S| + \frac{\delta_1}{k_1}\tilde{\rho}_1^2 + \frac{\delta_2}{k_2}\tilde{\rho}_2^2 + \frac{\delta_3}{k_3}\tilde{\rho}_3^2 \tag{32}$$

It is evident from the equation (32) that $\dot{V}_2 \le 0$. The parameter adaptive control law is stable.

The high-frequency buffeting phenomenon can be reduced by using the saturation function instead of the above symbolic function.

$$sat(S) = \begin{cases} 1 & S > \Delta \\ kS & |S| \le \Delta k = \frac{1}{\Delta} \\ -1 & S < -\Delta \end{cases} \tag{33}$$

The final control law is given in (29). ■

5. TORQUE OPTIMAL DISTRIBUTION

The objective in this section is to distribute the vertical torque optimally to the four wheels. In the design for torque control, the effective adhesion of each tire should be increased to maximum while satisfying the torque of

the control demand. The tire characteristics are shown in Figure 5. When the slip rate is zero, the lateral deflection is all produced by the side angle. In the relationship of friction circle, $\sqrt{F_{xi}^2+F_{yi}^2} \le \mu F_{zi}$, the longitudinal force of a tire is inversely proportional to its lateral force. When the longitudinal force reaches the attachment limit, it is indicated that the vehicle is prone to instability at the moment. Therefore, the smaller the adhesion and utilization of the tire, the more reasonable the torque distribution will be.

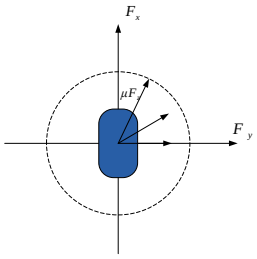

Fig. 5 tire characteristics during steering

The road adhesion utilization ratio of the tire is defined as the performance objective function (Li et al., 2016),

$$J=\sum_{i=1}^{4} C_i \frac{F_{xi}^2+F_{yi}^2}{(\mu F_{zi})^2} \tag{34}$$

Among them, i=1, 2, 3, 4 represents the front left wheel, the front right wheel, the rear left wheel and the rear right wheel, and the μ is the friction coefficient of the pavement. The C_i represents the weight coefficient, while F_{zi} is the vertical force.

The longitudinal force of the wheel is generally controlled directly in vehicle industry, and the effect of lateral force on the tire adhesion and utilization ratio is ignored. Thus, the objective function of the torque distribution is set as shown in (35) in this paper. The optimization is achieved by changing the longitudinal force of the wheel so that the utilization rate of the attached tire pavement is minimized.

$$J=\sum_{i=1}^{4} C_i \frac{F_{xi}^2}{(\mu F_{zi})^2} \tag{35}$$

According to the above simplified tire road adhesion utilization ratio, and $F_{xi}=\frac{T_{xi}}{R}$, the following torque based objective function for optimal torque distribution is finally obtained as below.

$$J=\sum_{i=1}^{4} C_i \frac{T_{xi}^2}{(\mu F_{zi} R)^2} \tag{36}$$

where $T_{xi}(i=1,2,3,4)$ is the total braking torque of a single wheel.

The Constraints in the optimization are discussed. According to the upper layer adaptive sliding mode stability controller, the yaw force and the total longitudinal force required for vehicle stability are calculated. The quantitative relationship between the longitudinal forces of the four wheels should satisfy the constraints of the upper moment with $cos\delta=1$,

$$\begin{cases} (F_{x1}+F_{x2})\cos\delta+F_{x3}+F_{x4}=ma_x \\ \frac{c}{2}(F_{x1}-F_{x2})\cos\delta+\frac{c}{2}(F_{x3}-F_{x4})=M_z \end{cases} \tag{37}$$

The equivalent expression of (37) in moment is as follows,

$$\begin{cases} (T_1+T_2)\cos\delta+T_3+T_4=T_q \\ \frac{c}{2R}(T_2-T_1)\cos\delta+\frac{c}{2R}(T_4-T_3)=M_z \end{cases} \tag{38}$$

The matrix form is,

$$Bu_c=v_c \tag{39}$$

where

$u_c=\begin{bmatrix} T_1 & T_2 & T_3 & T_4 \end{bmatrix}^T$, $B=\begin{bmatrix} 1 & 1 & 1 & 1 \\ -\frac{c}{2R} & \frac{c}{2R} & -\frac{c}{2R} & \frac{c}{2R} \end{bmatrix}$,

$v_c=\begin{bmatrix} T_q & M_z \end{bmatrix}^T$

The longitudinal force is bounded by the conditions of the adhesion of the pavement,

$$-\mu F_{zi} \le F_{xi} \le \mu F_{zi} \tag{40}$$

Or in the torque-based form,

$$-\mu F_{zi} R \le T_{xi} \le \mu F_{zi} R \tag{41}$$

The above constrained optimization control problem is of the quadratic programming standard form,

$$\begin{aligned} &\min_u J = u_c^T w u \\ &\text{sbuj.to} \\ &Aequ_c = Beq \\ &u_{\min} \le u_c \le u_{\max} \end{aligned} \tag{42}$$

The active set method for solving the quadratic programming problem is employed here. The Lagrange multiplier vector λ and μ are introduced, and the Lagrange function is as follows,

$$L(x,\lambda,\mu)=\frac{1}{2}u_c{}^T w u_c-\sum_{i=1}^{2}\lambda_i(B_i u_c-v_{ci})-\sum_{j=1}^{4}\mu_j(u_c-u) \tag{43}$$

The KKT condition that the optimal solution satisfies the global minimum is as follows,

$$\begin{cases}\sum_{i=1}^{2}\lambda_i B_i-\sum_{j=1}^{4}\mu_i=0\\ B_i u_c^*-v_{ci}=0,\lambda_i\ge 0\end{cases} \tag{44}$$

6. SIMULATION

In this paper, the developed stability control system and torque optimal distribution are evaluated by simulation under the computing environment of CarSim/Matlab, including a two DOF reference module, vehicle stability control module and torque distribution module. Among them, the vehicle stability control module of the adaptive sliding mode control is built in Matlab and the motor model is built in AMESim. Since the motor model is not the focus of this paper, the motor model building is not described in detail. The maximum motor torque references the motor parameters in the simulation software, ADVISOR2002, and the real-time motor speed uses the input to the Look-up-table module in Simulink, which gives the maximum motor torque at the current speed. Controller parameters used in the simulation is listed in Table 1.

Table 1 Controller parameters

parameter	name	Value
K_p	tracking error convergence rate to be determined in the design	8
K_s	moving speed at which any state moves toward the sliding surface	0.5
ξ	weight coefficient	0.2
K_1	adaptive gain of parameter ρ_1	1
K_2	adaptive gain of parameter ρ_2	0.6
K_3	adaptive gain of parameter ρ_3	0.9
δ_1	The undetermined coefficient of the estimated parameter ρ_1	20
δ_2	The undetermined coefficient of the estimated parameter ρ_2	25
δ_3	The undetermined coefficient of the estimated parameter ρ_3	30
Δ	Boundary layer	0.8

A lane changing simulation is designed using the module FMVSS126 in CarSim in conjunction with Matlab/Simulink. The developed adaptive sliding control method and the optimal torque distribution algorithm was evaluated. At the same time, a normal sliding mode method (without adaptation) has also been simulated and compared with the developed adaptive method. Two experiments have been conducted. In the first one, The simulation is carried out on the low adhesion coefficient road condition at $\mu=0.4$, and the initial speed set to 80km/h. The simulation results are shown in Fig. 6. From Fig. 6(h), we can see that the vertical load changes more obviously at t = 0-1.2s, as the vertical stiffness of the deflection is affected by the vertical load. The lateral stiffness is constantly changing, and the adaptive sliding mode controller controls the vehicle tracking the desired value of yaw rate and center of mass under the disturbance of the unbiased stiffness uncertainty. From Fig. 6(g), we can see that the optimized allocation of tire road adhesion utilization rate is small. The ground adhesion conditions are fully utilized. The torque distribution is reasonable, and the vehicle stability margin is large.

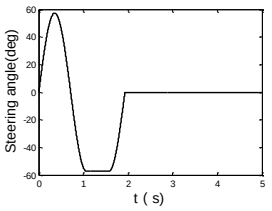

(a) Steering wheel angle input

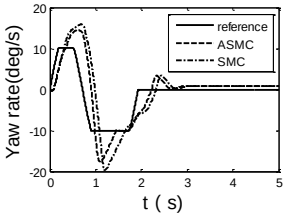

(b) Yaw rate comparison chart

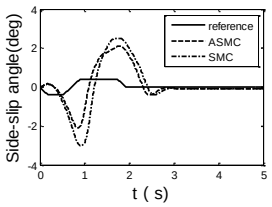

(c) Centroid off-angle comparison chart

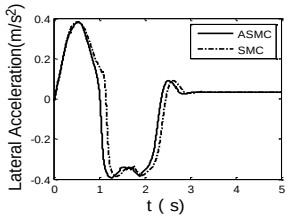

(d) Lateral acceleration comparison chart

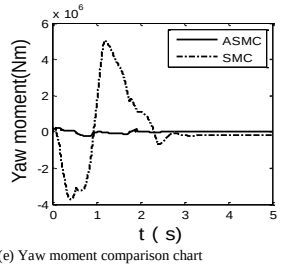

(e) Yaw moment comparison chart

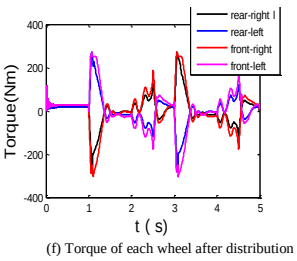

(f) Torque of each wheel after distribution

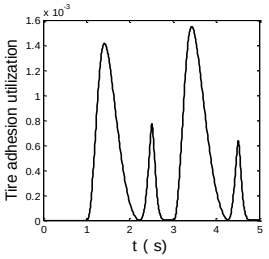

(g) Tire utilization rate

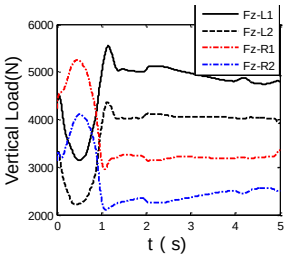

(h) Four wheel vertical force

Fig.6 Simulation results with low adhesion coefficient road condition at $\mu = 0.4$ and initial speed 80km/h

In the second experiment, the initial speed of the vehicle is set to 120km/h in Carsim, and the friction coefficient of the pavement is set to the dry road of $\mu = 0.85$. The results are shown in Fig.7. From the graph, we can see that the ordinary sliding mode controller has larger deviation of yaw rate and center sideslip angle, while the adaptive sliding mode control has smaller overshoot, which can better track the reference and control more effectively. From Fig. 7(g), it is shown that the utilization ratio of the tire pavement is small, which indicates that the adhesion performance of the tire is good.

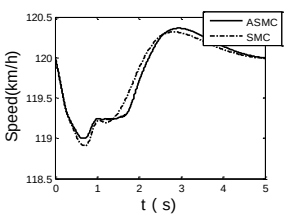

(a) Speed changes

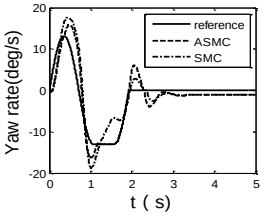

(b) Yaw rate comparison chart

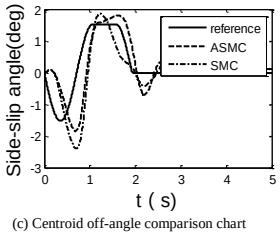

(c) Centroid off-angle comparison chart

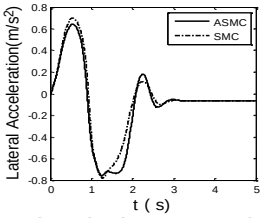

(d) Lateral acceleration comparison chart

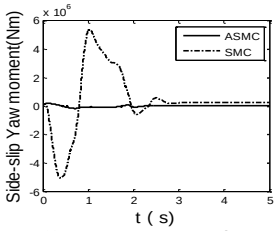

(e) Yaw moment comparison chart

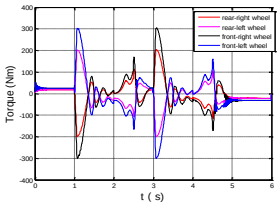

(f) Torque of each wheel after distribution

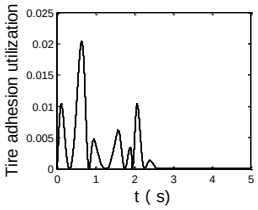

(g) Tire utilization rate

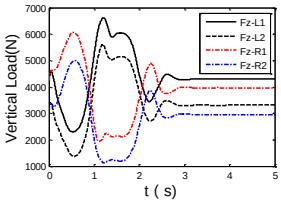

(h) Four wheel vertical force

Fig. 7 Simulation results with initial speed 120km/h and friction coefficient of the pavement of dry road $\mu = 0.85$

7. CONCLUSION

In this paper, an adaptive sliding mode control is proposed for four-wheel electric vehicles to solve the problem of parameter uncertainty in the vehicle stability control system. Lyapunov theory is used in derivation of the adaptive sliding mode control law so that the vehicle stability is guaranteed. Aiming at solving the problem of actuator redundancy, an optimal torque distribution method under constraints is proposed to improve the vehicle stability margin. Simulation results with CarSim/Matlab show that the proposed adaptive sliding mode control method has successfully coped with the model changes caused by vertical load transfer between front and rear axis, and is more effective than the ordinary fixed rate sliding mode control. The simulation also shows that the optimal torque distribution improves the vehicle stability margin. The next step in this research will be to estimate the center-of-mass declination. Then, a hardware-in-the-loop simulation will be carried out for further validation.

AKNOWLEDGEMENT

This project was supported by the national key Scientific Development Scheme of China, “Development and Innovation of Intelligent Assistant Driving Technology for Electric Cars” with Reference Number: JFYS 2016 ZY 02001610-02.

REFERENCES

Chiara, F. (2013). A review of energy consumption, management, and recovery in automotive systems, with considerations of future trends. *Proc. of the Institution of Mechanical Engineers Part D: Journal of Automobile Engineering*, **227 (06)**: 914-936.

Wolfgang Maiseh, et al. (2015). ABS5 and ASR5: The NEW ABS/ASR Family to Optimize Directional Stability and Traction. SAE930505.

Anh-Tuan Le, Chih-Keng Chen (2016). Vehicle stability control by using an adaptive sliding-mode algorithm.

International Journal of Vehicle Design, **72 (02)**, 107-131.

Milad Jalali (2017). Integrated model predictive control and velocity estimation of electric vehicles. *Mechatronics*, **46**, 84-100.

Hansung Lee (2009). Development of enhanced ESP system through vehicle parameter estimation. *Journal of Mechanical Science and Technology*, **23 (04),** 1046-1049.

Liang Lia, Gang Jia, Jie Chen (2015). A novel vehicle dynamics stability control algorithm based on the hierarchical strategy with constrain of nonlinear tire forces. *Vehicle System Dynamics*, **53(08)**: 1093-1116.

Wang, H., He, P., Yu, M. (2016). Adaptive neural network sliding mode control for steer-by-wire-based vehicle stability control. *Journal of Intelligent & Fuzzy Systems*, 885-902.

Choi, Mooryong, Choi, Seibum B. (2014). Model predictive control for vehicle yaw stability with practical concerns. *IEEE Trans. on Vehicular Technology*, **63(08)**: 3539-3548.

TCHAMNA, R. YOUN, I. (2013). Yaw rate and side-slip control considering vehicle longitudinal dynamics. *International Journal of Automotive Technology*, **14(01)**: 53-60.

EM RLER, M. T. (2015). Lateral stability control of fully electric vehicles. *International Journal of Automotive Technology*, **16(02),** 317-328.

Tsumasaka, A. (2009). Running stabilization control of electric vehicle based on cornering stiffness estimation. *Electrical Engineering in Japan*, **166(04),** 97-104.

Lian, Y. F. (2015). Cornering stiffness and sideslip angle estimation based on simplified lateral dynamic models for four-in-wheel-motor-driven electric vehicles with lateral tire force information. *International Journal of Automotive Technology*, **16(04)**: 669-683.

Kazemi, R. (2010). Nonlinear adaptive sliding mode control for vehicle handling improvement via steer-by-wire. *International Journal of Automotive Technology*, **11(03)**: 345-354.

Wang, Rongrong (2016). Robust H∞ Path Following Control for Autonomous Ground Vehicles With Delay and Data Dropout, 2016:1-9.

Hu, Chuan (2016). Robust H∞ output-feedback control for path following of autonomous ground vehicles. **70-71**: 414-427.

Zhiyong Zhang (2013). Observer-based H∞ control for vehicle handling and stability subject to parameter uncertainties. *J. Systems & Control Engineering*, **227(09)**: 704-717.

Yu, Zhuoping (2016). Direct yaw moment control for distributed drive electric vehicle handling performance improvement. *Chinese Journal of Mechanical Engineering*, **29(03)**: 486-497.

Hasan Alipour, Mehran Sabahi (2015). Lateral stabilization of a four wheel independent drive electric vehicle on slippery roads. *Mechatronics*, **30**: 275-285.

Zhao, Haiyan, Gao, Bingzhao (2015). Model predictive control allocation for stability improvement of four-wheel drive electric vehicles in critical driving condition. *IET Journal, Control Theory and Applications*, **09(18)**: 2688-2696.

Luo, Yugong, Cao, Kun, Yong Xiang (2015). Vehicle stability and attitude improvement through the coordinated control of longitudinal, lateral and vertical tyre forces for electric vehicles. *International Journal of Vehicle Design*, **69(1-4)**: 25-49.

Li, Bin, Goodarzi, Avesta (2015). An optimal torque distribution control strategy for four-independent wheel drive electric vehicles. *Vehicle System Dynamics*, **53(08)**: 1172-1189.

Kanghyun Nam (2014). Advanced Motion Control of Electric Vehicles Based on Robust Lateral Tire Force Control via Active Front Steering, *IEEE/ASME Transactions on Mechatronics*, **19(01)**: 289 - 299.

Kanghyun N. (2015). Design of an adaptive sliding mode controller for robust yaw stabilization of in-wheel-motor-driven electric vehicles[J]. *Int. Journal of Vehicle Design*, **67(01)**: 98 − 113.

Stratis, Kanarachos; Mohsen, Alirezaei (2014). Control allocation for regenerative braking of electric vehicles with an electric motor at the front axle using the state-dependent Riccati equation control technique. *Proceedings of the Institution of Mechanical Engineers. Part D: Journal of Automobile Engineering*, **228(02)**: 129-143.

Zhai, Li, Sun, Tianmin, Wang, Jie (2016). Electronic stability control based on motor driving and braking torque distribution for a four in-wheel motor drive electric vehicle. *IEEE Transactions on Vehicular Technology*, **65(06)**: 4726-4739.